materials

MDPI

Article

A Kinetic Model for the Modification of Al_2O_3 Inclusions during Calcium Treatment in High-Carbon Hard Wire Steel

Zuobing Xi, Changrong Li * and Linzhu Wang *

School of Material and Metallurgy, Guizhou University, Guiyang 550025, China; bingzxi@163.com
* Correspondence: author: crli@gzu.edu.cn (C.L.); lzwang@gzu.edu.cn (L.W.)

Abstract: Laboratory-scale experiments for the modification of Al_2O_3 inclusions by calcium treatment in high-carbon hard wire steel were performed and the compositions and morphological evolution of inclusions were studied. The kinetics of the modification of Al_2O_3 inclusions by calcium treatment were studied in high-carbon hard wire steel based on the unreacted shrinking core model, considering the transfer of Ca and Al through the boundary layer and within the product layer, coupled with thermodynamic equilibrium at the interfaces. The diffusion of Al in the inclusion layer was the limiting link in the inclusion modification process. The Ca concentration in molten steel had the greatest influence on the inclusion modification time. The modification time for inclusions tended to be longer in the transformation of higher CaO-containing calcium aluminate. The modification of Al_2O_3 into CA_6 was fastest, while the most time was needed to modify CA into $C_{12}A_7$. It took about six times time longer at the later stage of inclusion modification than at the early stage. The complete modification time for inclusions increased with the square of their radii. The changes of CaO contents with melting time were estimated based on a kinetic model and was consistent with experimental results.

Keywords: high-carbon hard wire steels; inclusions; calcium treatment; unreacted shrinking core model

Citation: Xi, Z.; Li, C.; Wang, L. A Kinetic Model for the Modification of Al_2O_3 Inclusions during Calcium Treatment in High-Carbon Hard Wire Steel. *Materials* **2021**, *14*, 1305. https://doi.org/10.3390/ma14051305

Academic Editor: Federico Mazzucato

Received: 1 February 2021
Accepted: 2 March 2021
Published: 9 March 2021

1. Introduction

High-carbon hard wire steels are mainly applied in massive engineering projects such as bridges, cables, airports, power stations, and dams [1–3]. High-carbon hard wire products are drawn into filaments with a diameter of about 5 mm [4,5]. The hard inclusions with large sizes affect the steel yield and performance. Al_2O_3 inclusions are brittle with high melting temperatures, which are the major factors believed to impact the performance of high-carbon hard wire steels [6]. Therefore, Ca is usually used to modify Al_2O_3 inclusions to improve the performance of high-carbon hard wire steels.

Calcium treatment is one of the most commonly used and effective methods for modifying non-metallic inclusions into liquid ones [7–10]. The solid alumina can be converted into calcium aluminate inclusions partially or completely during calcium treatment [11,12], reducing the blockage of the immersion nozzle during continuous casting [10,13]. Since the 1990s, many studies have been conducted to understand the modification mechanism for alumina inclusions using calcium treatment [9,14–16]. Research studies on the modification kinetics for Al_2O_3 inclusions have been conducted in order to evaluate the accurate addition amounts for calcium and to understand the modification evolution process. Lu et al. [17] first established the kinetic model for oxide and sulfide inclusions in the calcium treatment process. They assumed that the internal diffusion rate of the inclusions is extremely fast and the interface reaction is rapid, and they developed an inclusion evolution model. Higuchi et al. [18] revised the kinetic model for modification of Al_2O_3 inclusions by using a first-order reaction equation. They studied the gasification rate of calcium from the melt and the reaction rate between the melt and inclusions. In this model, they assumed that the size and number of inclusions remained constant. Visseret al. [19] divided the ladle into two reaction zones: one is a high-calcium and low-oxygen zone, while the

other is a low-calcium and low-oxygen zone. The kinetics of calcium treatment in the ladle stage was simulated, in which the results were in agreement with the experimental results. Ito et al. [20] studied the factors affecting the kinetics of calcium treatment using laboratory experiments. The modification of inclusions by calcium treatment was improved by shortening the aluminum deoxidation time, increasing the gas stirring, and increasing the reaction time after calcium treatment. They compared the calculated results based on the unreacted nucleus model and experimental results, and then proposed that the limiting link for the inclusion modification reaction is the mass transfer process in the product layer. Han et al. [21] believed that the decisive step is the chemical reaction rate between alumina and liquid calcium aluminate. Park et al. [22] believed that Al_2O_3 inclusions can be treated as unreacted nuclei at the beginning of modification and that the limiting link of the modification process is the diffusion of Al in the inclusion layer. However, they only discussed the rationality of the model, while a complete dynamic model has not yet been established. Zhang et al. [12] proposed a kinetic model of inclusion modification, considering the reduction of calcium in slag, the calcium dissolution rate in steel, mass transfer in the boundary layer, and solute diffusion in the product layer. The transformation model for alumina to magnesia–alumina spinel inclusions was established by Galindo et al. [23], and it was found that the transformation of inclusions was affected by the reaction at the slag–metal interface. Tabatabaei et al. [24] developed a kinetic model of inclusion transformation, which was applied to study the slag–steel reaction in a ladle furnace and to predict the composition changes for steel and slag and the evolution of inclusions during Ca treatment. Turkdogan et al. [25] found that the size of inclusions affected the modification rate, whereby large-sized inclusions were more difficult to modify than small-sized inclusions. Ye et al. [26] and Zheng et al. [14] proposed that with the increase in the calcium content in molten steel, the modification route was:

$$Al_2O_3 \rightarrow CaO \cdot 6Al_2O_3(CA_6) \rightarrow CaO \cdot 2Al_2O_3(CA_2) \rightarrow CaO \cdot Al_2O_3(CA) \rightarrow 12CaO \cdot 7Al_2O_3(C_{12}A_7) \rightarrow 3CaO \cdot Al_2O_3(C_3A) \quad (1)$$

Numerical simulation has many advantages, such as operating at low temperatures, having good reproducibility, being low cost, and detailed experimental data being available. Therefore, more metallurgical workers are using numerical simulation methods to study the behavior of inclusions in steel, and then to obtain the variation law for each parameter in the process and the quantitative relationships between each parameter [27].

On the basis of the multilayer unreacted core model for alumina inclusions, a step-by-step reaction kinetic model for the modification of Al_2O_3 inclusions by calcium treatment in high-carbon hard wire steel was established. The effects of Al, Ca, and O contents on the modification of high-carbon hard wire steel was studied during calcium treatment. The conversion ratio, radii of inclusions, calcium oxide contents in inclusions, and modification times were predicted. This work is helpful for understanding the inclusion modification process and for improving calcium treatment technology.

2. Experiment

2.1. Experimental Procedure

The tested steels were produced based on the chemical compositions of SWRH62A steel. Two heat experiments with different amount of deoxidants (A and B) were carried out in a tubular resistance furnace, as shown in Figure 1. The corundum crucible containing about 400 g pure iron, ferrosilicon alloy, and electrolytic manganese was placed in the furnace. Table 1 lists the compositions of raw materials used in the study. The temperature was increased to 1600 °C using electric heating. The added alloys and sampling procedures used in the experiments are shown in Figure 2. The aluminum alloy and Si–Ca alloy were added to the liquid steel for deoxidation at certain times. Calcium treatment was carried out after Al deoxidization. Four samples were sucked out using a quartz tube (ϕ 5 mm) and then quenched by insertion into a sodium chloride solution at different times after calcium addition (60, 180, 600, and 720 s). During the steel smelting process, the argon gas flow rate was maintained at 5 min/L.

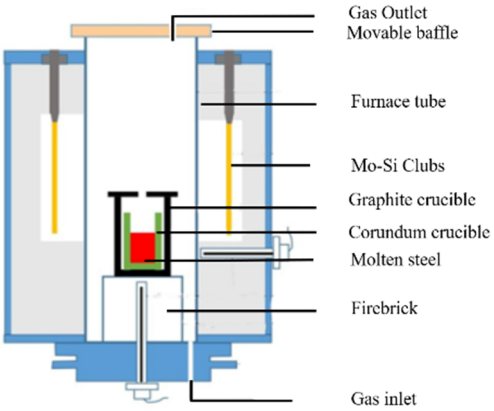

Figure 1. Schematic of tube furnace used in experiments. Reprinted with permission from [28]

Table 1. Compositions of raw materials (mass%).

Raw material	Fe	Si	Mn	S	C	Ca	Al	Others
Industrial pure iron	99.7	0.02	0.03	0.0002	0.0018	-	0.001	0.2445
Electrolytic manganese	-	-	99.999	-	-	-	-	0.001
Si–Fe alloy	21	78	0.4	0.02	0.1	-	-	0.48
Al alloy	0.7	0.8	0.15	-	-	-	96.94	1.41
Si–Ca alloy	-	57.13	20.44	-	0.83	19.56	2.02	0.02
QT400	95.8	0.17	0.5	0.01	3.45	-	-	0.07

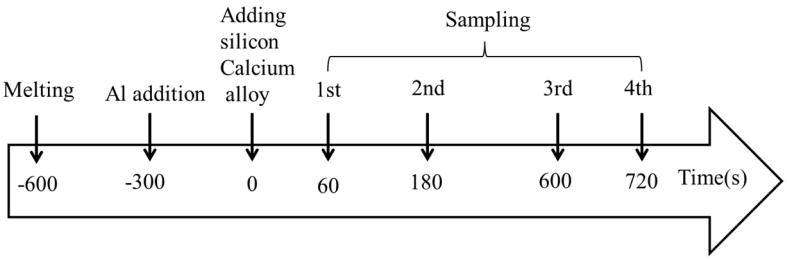

Figure 2. Addition of alloys and sampling procedure used in current experiments.

2.2. Composition Analysis for Steels and Inclusions

The contents of calcium and aluminum in experimental steels were assessed using inductively coupled plasma–mass spectrometry (ICP–MS, Su Zhou, China) The contents of C, Si, Mn, and S in experimental steels were assessed using a direct-reading spectrometer (Q4-TASMAN, Brooke, Germany). The O contents in experimental steels were assessed using an inorganic oxygen–hydrogen tester.

The metallographic samples were ground using abrasive papers and then polished. The two-dimensional morphologies and compositions of inclusions in a cross section of each sample were analyzed using scanning election microscopy (ZeissΣIGMA+ X-Max20, Baden-Wurttemberg, Germany) and energy-dispersive spectrometry. About 30 inclusions were detected in each sample.

3. Results

3.1. Chemical Compositions of Steels

Table 2 lists the measured compositions of steels. A significant difference was found in the mass fractions of calcium between the two experiments due to the different amounts of Si-Ca alloy added. This showed that steel A had a high calcium content of 0.0025 mass%, while steel B had a low calcium content of 0.0017 mass%.

Table 2. Chemical compositions of steels used in different experiments (mass%).

Number	C	Si	Mn	S	O	Al	Ca
A	0.652	0.183	0.312	0.0021	0.0051	0.0042	0.0025
B	0.652	0.183	0.300	0.0017	0.0061	0.0038	0.0017

3.2. Compositions and Morphologies of Inclusions

The compositions of inclusions detected at 60, 180, 600, and 720 s after calcium addition are shown in Figure 3. The mass fractions of CaO in calcium aluminate inclusions were in the range of 7.75–29.23% at 60 s after calcium addition and the average mass fraction of CaO was 19.22% in steel A. This indicates that the main types of inclusions were CA_6 and CA_2 in steel A. The average mass fractions of CaO in calcium aluminate inclusions in steel A increased to 40.17%, 50.05%, and 60.43% after adding calcium for 180, 600, and 720 s, respectively. This indicates that the inclusions were modified into CA + $C_{12}A_7$, $C_{12}A_7$, and $C_{12}A_7$ + C_3A gradually with the prolonging of the calcium treatment time. The mass fraction of CaO in calcium aluminate inclusions for steel B was less than that in steel A. The average mass fractions of CaO in calcium aluminate inclusions in steel B increased to 9.09%, 20.04%, 32.53%, and 40.12% after adding calcium for 60, 180, 600, and 720 s, respectively. This indicates that the inclusions were modified into CA_6, CA_6 + CA_2, CA_2 + CA, and CA + $C_{12}A_7$ gradually with the prolonging of the calcium treatment time.

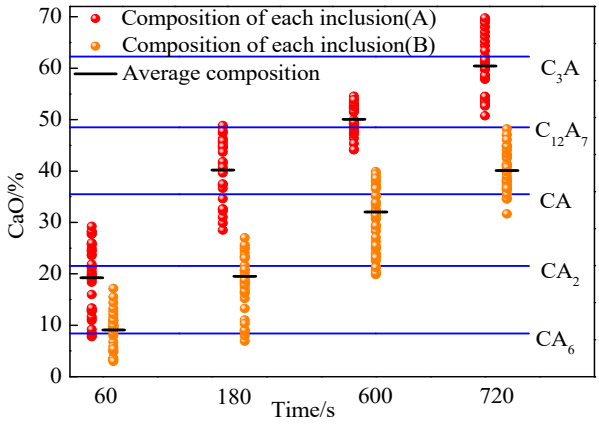

Figure 3. Compositions of inclusions detected in experiment steels (A and B) after calcium addition.

The compositions, morphologies, and elemental mappings of typical inclusions detected in samples after calcium addition are shown in Figure 4 (steel A) and Figure 5 (steel B). Figure 4a shows that the typical inclusion $CaO{\cdot}2Al_2O_3$ that formed after calcium treatment for 60 s was irregular in steel A. The $CaO{\cdot}Al_2O_3$ that formed after calcium treatment for 180 s was similar to a hexagon, of which the edges tended to be smooth. Typical inclusions $12CaO{\cdot}7Al_2O_3$ and $3CaO{\cdot}Al_2O_3$ occurred in steel A at later stages of deoxidation and their morphologies tended to be spherical. Figure 4a shows the typical inclusions of $CaO{\cdot}6Al_2O_3$, $3CaO{\cdot}8Al_2O_3$, $CaO{\cdot}2Al_2O_3$, and $CaO{\cdot}Al_2O_3$ formed in steel B after calcium treatment for 60, 180, 600, and 720 s, respectively. Their morphologies were irregular and their sharp corners tended to be disappeared.

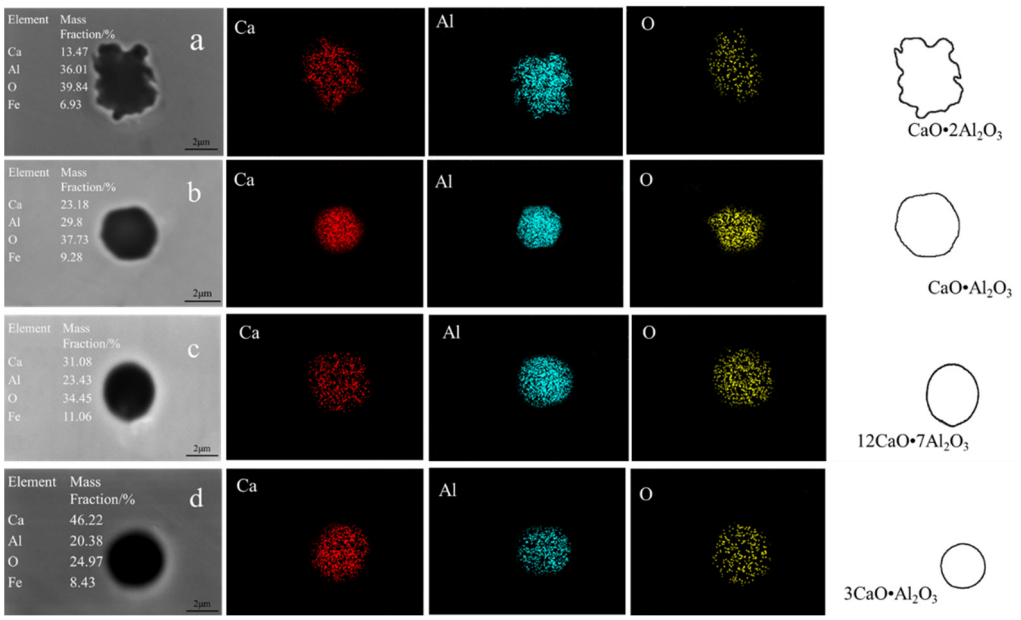

Figure 4. Elemental mappings of different types of inclusions detected after calcium additions in steel A: (**a**) 60 s; (**b**) 180 s; (**c**) 600 s; (**d**) 720 s.

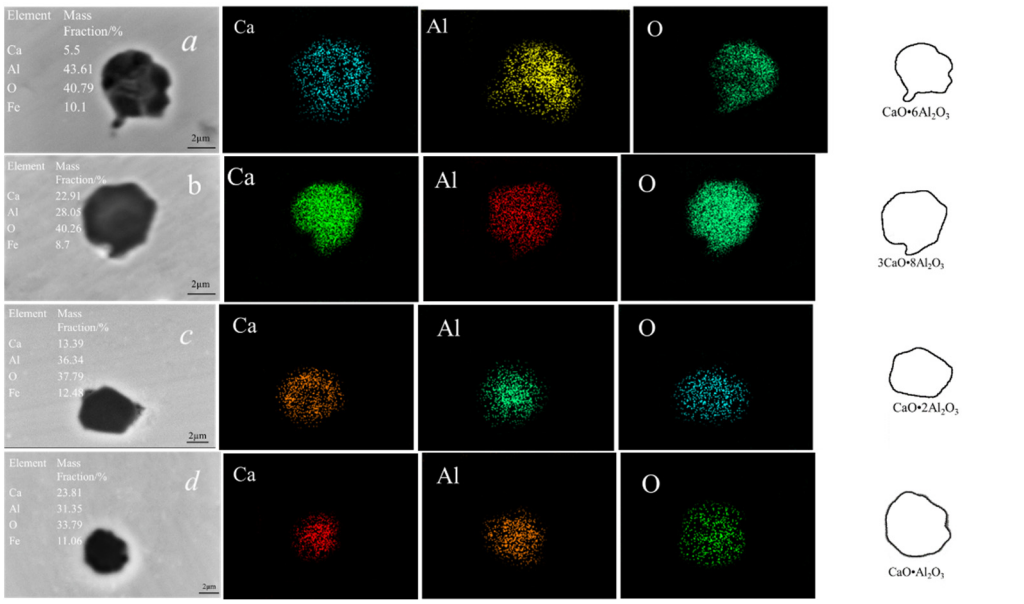

Figure 5. Elemental mappings of different types of inclusions detected after calcium additions in steel B: (**a**) 60 s; (**b**) 180 s; (**c**) 600 s; (**d**) 720 s.

4. Discussion

4.1. Dynamic Model

The mass transfer process and modification of Al_2O_3 inclusions in high-carbon hard wire steels can be described by the unreacted core model shown in Figure 6 based on experimental results. The modification process of Al_2O_3 inclusions can be described as shown in Figure 6 based on experimental results. The Al_2O_3 inclusion wrapped in the CA_6 layer formed at the start of calcium treatment and Ca transferred into the unreacted core of Al_2O_3 through the CA_6 layer. Therefore, the unreacted core of Al_2O_3 gradually decreased and the CA_6 layer gradually thickened, then Al_2O_3 inclusions transformed into CA_6 completely. With the diffusion of Ca and its increasing content, a complex inclusion with a core of CA_6 wrapped in a CA_2 layer formed and Ca transferred from the product

layer (CA_6 layer) to boundary layer (the interface between CA_2 and CA_6), resulting in the formation of a spherical inclusion with CA_2. Similarly, the CA_2 was transformed into CA, $C_{12}A_7$, and C_3A step-by-step with the transfer of Ca and the chemical reaction between calcium aluminates. The assumptions in the current model are as follows:

1. All inclusions in molten steel are spherical before and during the calcium treatment process;
2. The temperature of molten steel is very high at 1600 °C, so the interfacial reaction is assumed to be in equilibrium;
3. To simplify the discussion of the model, the concentrations of calcium, aluminum, and oxygen in molten steel are assumed to be constant;
4. The diffusion of all substances in the liquid calcium aluminate layer is steady, which is in accordance with Fick's first law.

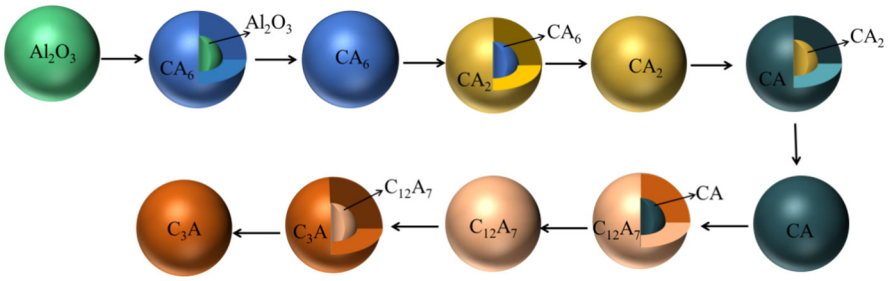

Figure 6. Kinetic model of alumina inclusions in calcium-modified steel.

Taking the transformation of CA inclusions into $C_{12}A_7$ as an example, the process is divided into the following three steps.

1. Ca in molten steel diffuses to the $C_{12}A_7$ layer–molten steel interface, for which the reaction formula is:

$$Ca_{(s)} \rightarrow [Ca]_{(l)} \quad (2)$$

Ca passes through the $C_{12}A_7$ liquid phase, diffuses to the CA layer, and reacts with it:

$$15[Ca] + 33(CaO \cdot Al_2O_3)_{(s)} = 4(12CaO \cdot 7Al_2O_3)_{(s)} + 10[Al] \quad (3)$$

2. At this time, the generated [Al] diffuses outward through the $C_{12}A_7$ liquid phase layer and enters into the molten steel.

Figure 7 is a schematic of the transformation process of $CaO{\cdot}Al_2O_3$ into $12CaO{\cdot}7Al_2O_3$ inclusions. In the Figure 7, r_0 represents the radius of $C_{12}A_7$ inclusion after complete modification, r represents the radius of the unreacted CA inclusion, and l_1 and l_2 represent the interface between CA inclusion and $C_{12}A_7$ inclusions, respectively. In the refining process, argon blowing and stirring are used. (Ca) and (Al) diffuse rapidly in molten steel and in the high-temperature reaction process. Therefore, the rate control link in the modification process for inclusions is solute diffusion in the calcium aluminate layer. At 1600 °C, the diffusion coefficients of Ca and Al in the calcium aluminate layer are [24,29] $D_{Ca} \approx 10^{-8.6}$ $m^2{\cdot}s^{-1}$ and $D_{Al} \approx 10^{-10.4}$ $m^2{\cdot}s^{-1}$, respectively. In this paper, the kinetics of the Al_2O_3 inclusion modification in high-carbon hard wire steel were analyzed in two cases. In the first case, the diffusion process of Al in the calcium aluminate layer was the limiting link. In the second case, the diffusion of Ca in the calcium aluminate layer was the limiting link in the process of inclusion modification.

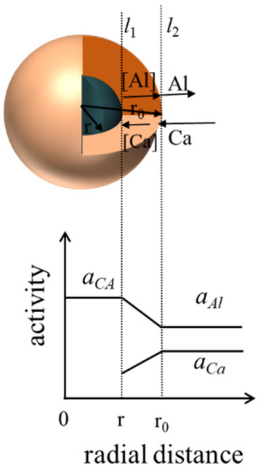

Figure 7. Schematic of the transformation of CA inclusions into $C_{12}A_7$ inclusions. (l_1 represents the interface layer between CA and $C_{12}A_7$ inclusions, l_2 represent that surface layer between the $C_{12}A_7$ inclusion and the molten steel boundary, a_{CA} indicates the activity of CA inclusions, a_{Al} indicates the activity of Al, a_{Ca} indicates the activity of Ca).

When the diffusion of Al in the calcium aluminate layer is the limiting link in inclusion modification, the diffusion rate of Al in the $C_{12}A_7$ layer is expressed as:

$$v_{Al} = -\frac{dn_{Al}}{dt} = 4\pi r^2 D_{Al}\frac{dc_{Al}}{dr} \tag{4}$$

where n_{Al} represents the amount of Al, r represents the radius of unreacted nuclear CA, D_{Al} indicates the diffusion rate of Al in molten steel, c_{Al} is the concentration of Al in $C_{12}A_7$, and t represents the modification time of inclusions:

$$dc_{Al} = -\frac{1}{4\pi D_{Al}}\frac{dn_{Al}}{dt}\frac{dr}{r^2} \tag{5}$$

Equation (5) is integrated as:

$$\int_{C_{Al,l_1}}^{C_{Al,l_2}} dc_{Al} = -\frac{1}{4\pi r^2 D_{Al}}\frac{dn_{Al}}{dt}\int_r^{r_0}\frac{dr}{r^2} \tag{6}$$

From Equation (6), we get:

$$v_{Al} = -\frac{dn_{Al}}{dt} = 4\pi D_{Al}\frac{r_0 r}{r_0 - r}(c_{Al,l_1} - c_{Al,l_2}) \tag{7}$$

In the formula, c_{Al,l_1} represents the Al concentration at the interface between two inclusions and c_{Al,l_2} represents the Al concentration at the interface between inclusion $C_{12}A_7$ and molten steel.

According to Equation (7), the rate of Al consumption in the modification reaction is:

$$-\frac{dn_{Al}}{dt} = -\frac{2dn_{Al_2O_3}}{dt} = -\frac{x_{Al_2O_3}dn_{CA}}{dt} = -\frac{51}{79}\frac{4\pi r^2\rho_{CA}}{M_{CA}}\frac{dr}{dt} \tag{8}$$

where ρ_{CA} represents the density of CA, $\rho_{CA} = 2.96 \times 10^3$ kg/m^3, and M_{CA} represents the molar mass of CA, M_{CA}=158g/mol.

Combining Equation (7) with Equation (8), we can obtain:

$$\int_0^t \frac{79M_{CA}D_{Al}(c_{Al,l_1} - c_{Al,l_2})}{51\rho_{CA}}dt = \int_{r_0}^{r}(r - \frac{r^2}{r_0})dr \tag{9}$$

The relationship between the unreacted nucleus radii of inclusions and the modification time (t) can be obtained by finishing the following:

$$t = \frac{17\rho_{CA}r_0^2}{158M_{CA}D_{Al}(c_{Al,l_1} - c_{Al,l_2})}\left[1 - 3(\frac{r}{r_0})^2 + 2(\frac{r}{r_0})^3\right] \quad (10)$$

To calculate the modification time of inclusions, the activity of solute elements in steel was used instead of its concentration. Equation (10) can be expressed as:

$$t = \frac{17\rho_{CA}r_0^2}{158M_{CA}D_{Al}(a_{Al,l_1} - a_{Al,l_2})}\left[1 - 3(\frac{r}{r_0})^2 + 2(\frac{r}{r_0})^3\right] \quad (11)$$

When CA inclusions are completely transformed into $C_{12}A_7$, when $r = 0$, the complete modification time (t_f) of inclusions is:

$$t_f = \frac{17\rho_{CA}r_0^2}{158M_{CA}D_{Al}(a_{Al,l_1} - a_{Al,l_2})} \quad (12)$$

where ρ_{CA}, M_{CA}, and D_{Al} are all constants and the modification time for CA inclusions depends on their radii and the activity difference of Al between the interface between two inclusions and the interface between molten steel and inclusions.

When the diffusion of Ca in the calcium aluminate layer is the limiting link in inclusion modification, the diffusion rate of Ca in the $C_{12}A_7$ layer is expressed as follows:

$$v_{Ca} = \frac{dn_{\mathrm{Ca}}}{dt} = 4\pi r^2 D_{\mathrm{Ca}}\frac{dc_{\mathrm{Ca}}}{dr} \quad (13)$$

where n_{Ca} represents the amount of Ca, r represents the radius of unreacted nuclear CA, D_{Ca} indicates the diffusion rate of Ca in molten steel, c_{Ca} is the concentration of Ca in $C_{12}A_7$, and t represents the modification time of inclusions:

$$dc_{Ca} = \frac{1}{4\pi D_{\mathrm{Ca}}}\frac{dn_{\mathrm{Ca}}}{dt}\frac{dr}{r^2} \quad (14)$$

Equation (14) is integrated as:

$$\int_{C_{\mathrm{Ca},l_1}}^{C_{\mathrm{Ca},l_2}} dc_{\mathrm{Ca}} = \frac{1}{4\pi r^2 D_{\mathrm{Ca}}}\frac{dn_{\mathrm{Ca}}}{dt}\int_r^{r_0}\frac{dr}{r^2} \quad (15)$$

From Equation (15), we get:

$$v_{Ca} = \frac{dn_{\mathrm{Ca}}}{dt} = 4\pi D_{\mathrm{Ca}}\frac{r_0 r}{r_0 - r}(c_{\mathrm{Ca},l_1} - c_{\mathrm{Ca},l_2}) \quad (16)$$

In the formula, c_{Ca,l_1} represents the Ca concentration at the interface between two inclusions and c_{Ca,l_2} represents the Ca concentration at the interface between inclusion $C_{12}A_7$ and molten steel.

The rate of Ca generated by the modification reaction is:

$$\frac{dn_{\mathrm{Ca}}}{dt} = \frac{2dn_{CaO}}{dt} = \frac{x_{CaO}dn_{C_{12}A_7}}{dt} = \frac{16}{33}\frac{4\pi r^2\rho_{C_{12}A_7}}{M_{C_{12}A_7}}\frac{dr}{dt} \quad (17)$$

where $\rho_{C_{12}A_7}$ represents the density of $C_{12}A_7$, $\rho_{C_{12}A_7}$ = 2.83 × 10^3 kg/m^3, and $M_{C_{12}A_7}$ represents the molar mass of $C_{12}A_7$, $M_{C_{12}A_7}$ = 1386g/mol.

Combining Equation (16) with Equation (17), we can obtain:

$$\int_0^t \frac{33M_{C_{12}A_7}D_{\mathrm{Ca}}(c_{Ca,l_1} - c_{Ca,l_2})}{16\rho_{CA}}dt = \int_{r_0}^{r}(r - \frac{r^2}{r_0})dr \quad (18)$$

The relationship between unreacted nucleus radii of inclusions and modification time (t) can be obtained by finishing:

$$t = \frac{8\rho_{C_{12}A_7} r_0^2}{99 M_{C_{12}A_7} D_{\mathrm{Ca}} (c_{Ca,l_1} - c_{Ca,l_2})} \left[1 - 3\left(\frac{r}{r_0}\right)^2 + 2\left(\frac{r}{r_0}\right)^3\right] \tag{19}$$

To calculate the modification time of the inclusions, the activity of solute elements in steel was used instead of its concentration. Equation (18) can be expressed as:

$$t = \frac{8\rho_{C_{12}A_7} r_0^2}{99 M_{C_{12}A_7} D_{\mathrm{Ca}} (a_{Ca,l_1} - a_{Ca,l_2})} \left[1 - 3\left(\frac{r}{r_0}\right)^2 + 2\left(\frac{r}{r_0}\right)^3\right] \tag{20}$$

When CA inclusions are completely transformed into $C_{12}A_7$, when $r = 0$, the complete modification time (t_f) of inclusions is:

$$t_f = \frac{8\rho_{C_{12}A_7} r_0^2}{99 M_{C_{12}A_7} D_{\mathrm{Ca}} (a_{Ca,l_1} - a_{Ca,l_2})} \tag{21}$$

where $\rho_{C_{12}A_7}$, $M_{C_{12}A_7}$, and D_{Ca} are all constants, and the modification time of CA inclusions depends on their radius and the activity difference of Ca between the interface between two inclusions and the interface between molten steel and inclusions.

4.2. Model and Parameter Determination

When the diffusion of Al in the calcium aluminate layer is the limiting link in inclusion modification, the concentration of [Al] in calcium aluminate inclusions is difficult to determine and can be replaced by a_{Al} as the following formula:

For interface l_1:

$$15[\mathrm{Ca}] + 33(\mathrm{CaO} \cdot \mathrm{Al_2O_3})_{(\mathrm{s})} = 4(12\mathrm{CaO} \cdot 7\mathrm{Al_2O_3})_{(\mathrm{s})} + 10[\mathrm{Al}] \tag{22}$$

The Gibbs free energy of this reaction is [25,29,30]:

$$\Delta G_1^{\theta} = -565,555 - 1609.66T, \mathrm{J} \cdot \mathrm{mol}^{-1} \tag{23}$$

$$\Delta {G_1}^{\theta} = -RT \ln K^{\theta} = -RT \ln \frac{a_{Al,l_1}^{10} a_{12CaO \cdot 7Al_2O_3}^{4}}{a_{Ca}^{15} a_{CaO \cdot Al_2O_3}^{33}} \tag{24}$$

$$a_{Al,l_1} = \left[\frac{a_{Ca}^{15} a_{CaO \cdot Al_2O_3}^{33}}{a_{12CaO \cdot 7Al_2O_3}^{4}} \exp\left(\frac{\Delta {G_1}^{\theta}}{-RT}\right)\right]^{\frac{1}{10}} \tag{25}$$

In the formula, a_{Al,l_1} represents the activity of the interface layer Al between inclusion CA and $C_{12}A_7$, while $a_{CaO \cdot Al_2O_3}$ and $a_{12CaO \cdot 7Al_2O_3}$ are regarded as 1:

$$a_i = f_i \times [\%i] \tag{26}$$

$$a_{Al,l_2} = f_{Al} \times [\%\mathrm{Al}] \tag{27}$$

where a_{Al,l_2} represents the activity of Al at the interface between $C_{12}A_7$ inclusions and molten steel.

When the diffusion of Ca in the calcium aluminate layer is the limiting link in inclusion modification, the activity of the interface layer Ca between inclusion CA and $C_{12}A_7$ can be estimated as Equation (28).

For interface l_1:

$$a_{Ca,l_1} = \left[\frac{a_{Al}^{10} a_{12CaO\cdot 7Al_2O_3}^{4}}{a_{CaO\cdot Al_2O_3}^{33} \exp\left(\frac{\Delta G_1^{\theta}}{-RT}\right)} \right]^{\frac{1}{15}} \quad (28)$$

In the formula, a_{Ca,l_1} represents the activity of the interface layer Ca between inclusion CA and $C_{12}A_7$, while $a_{CaO\cdot Al_2O_3}$ and $a_{12CaO\cdot 7Al_2O_3}$ are regarded as 1.

For interface l_2:

$$a_{Ca,l_2} = f_{Ca} \times [\%Ca] \quad (29)$$

The formula shows the activity of Ca at the interface between $C_{12}A_7$ inclusions and molten steel.

According to the interface shown in Equation (13), combined with the experimental steel composition in Table 2 and the interaction coefficient between elements in molten steel at 1873 K as shown in Table 3.

Table 3. Interaction coefficients of Ca, O, and Al in molten steel at 1873 K (1600 °C) [13,31,32].

e_i^j	C	Si	Mn	S	Al	O	Ca
Ca	−0.34	−0.095	−0.007	−28	−0.072	−780	−0.002
O	−0.42	−0.066	−0.021	−0.13	−1.17	−0.17	−313
Al	0.091	0.056	−0.004	0.035	−0.043	−1.98	−0.047

Equation (17) was used to calculate the activities of Ca and Al in each test steel (as shown in Table 4).

Table 4. Activity of Ca and Al in steel A and steel B.

Steel	a_{Ca}	a_{Al}
A	1.31×10^{-7}	0.0048
B	1.52×10^{-8}	0.0043

4.3. Determination of Restrictive Links

According to Equations (12) and (21), the diffusion of Al and Ca in the $C_{12}A_7$ layer, which treated as limiting link in the transformation of CA inclusions into $C_{12}A_7$ in steel A, was calculated as shown in Figure 8. It can be seen that the value of t_f is larger in the red line than that in the black line when the radius is same. This indicates that the diffusion of Al in the inclusion layer was the limiting link in the modification process of inclusions, which was consistent with the research results of Park et al. [24].

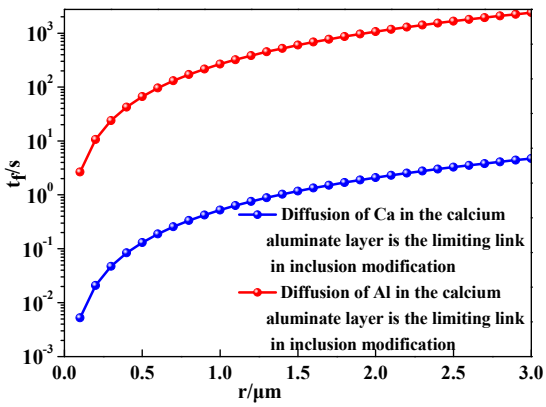

Figure 8. Diffusion of Ca and Al in the calcium aluminate layer is the limiting link of modification.

4.4. Effects of Solute Element Content in Molten Steel on Modification Time

The modification of inclusions depends on the activity of Al, which is affected by the content of each solute element in molten steel. The effects of Ca, Al, and O contents in molten steel on the time taken to modify CA into $C_{12}A_7$ inclusions with a radius of 1.5 μm was studied based on Equations (12), (25), and (27), as shown in Figure 9. The modification time increased linearly with increasing oxygen content and decreased with increasing calcium content in molten steel. When the content of O increased in the range of 0.0002–0.0045%, the modification time was prolonged from 0.0011 s to 118 s, increasing by approximately 118 s. When the content of Ca increased in the range of 0.0002–0.0045%, the modification time for complete transformation of Ca inclusions into $C_{12}A_7$ was reduced from 48616 s to 247 s, which was reduced by approximately 48369 s. The change of modification time with increasing Al content was very small. It can be seen that the Ca concentration in molten steel had the greatest influence on the modification time of inclusions. The steel with high Ca content was favorable for the modification of CA inclusions into $C_{12}A_7$ inclusions.

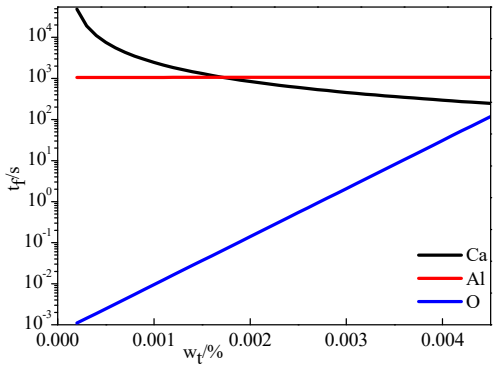

Figure 9. Effects of solute element content in molten steel on the time of complete modification of CA inclusions into $C_{12}A_7$.

The relationship between the Ca content in molten steel and modification time of inclusions was calculated based on Equations (12) and (25), as shown in Figure 10. The complete modification time for inclusions was significantly shortened with the increase of the Ca content in molten steel and decrease of the inclusion radius. When the Ca content in molten steel was 0.0025% and the radius of inclusion was 1.5 μm, the modification times for Al_2O_3 into CA_6, CA_6 into CA_2, CA_2 into CA, CA into $C_{12}A_7$, and $C_{12}A_7$ into C_3A were 4.5, 16, 116, 601, and 449 s, respectively. This indicates that the modification times for inclusions tend to be longer in the transformation of higher CaO-containing calcium aluminate. The modification of Al_2O_3 into CA_6 was fastest, while the most time was required to modify CA into $C_{12}A_7$. When calcium aluminate inclusions changed from solid state to liquid state, this process was the most difficult to carry out and the required modification time was the longest.

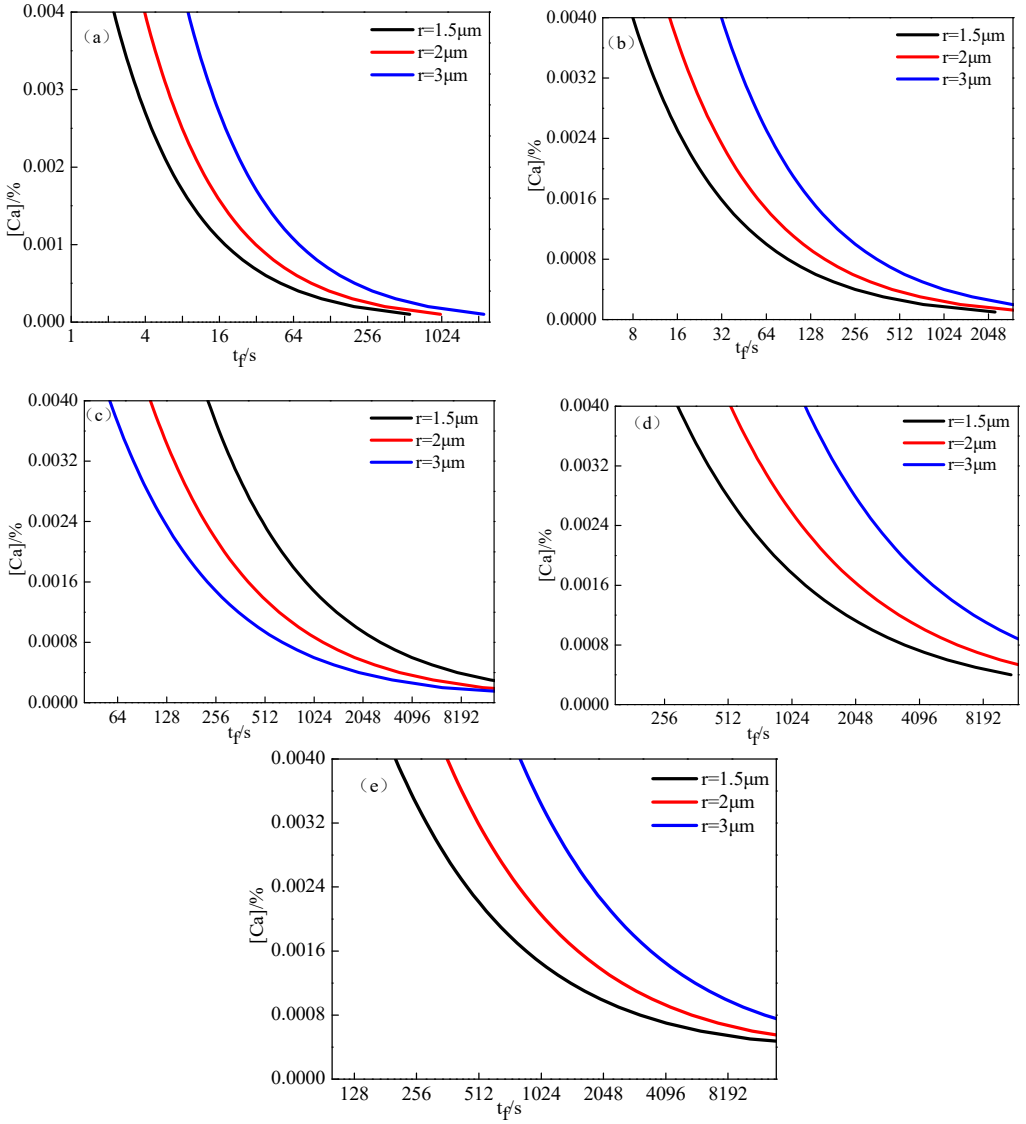

Figure 10. Relationship between Ca content in molten steel and complete modification times for inclusions with different compositions: (**a**) Al_2O_3 modified into CA_6; (**b**) CA_6 modified into CA_2; (**c**) CA_2 modified into CA; (**d**) CA modified into $C_{12}A_7$; (**e**) $C_{12}A_7$ modified into C_3A.

4.5. Influence of Inclusion Conversion Rate in Molten Steel on Modification Time

In order to evaluate the modification rate, taking CA to $C_{12}A_7$ as an example, the inclusion conversion ratio is defined as:

$$\alpha = \frac{m_{CA(\text{Initial})} - m_{CA(\text{End})}}{m_{CA(\text{Initial})}} \times 100\% \quad (30)$$

According to Equations (11) and (30), the relationship between the conversion ratio and modification time during inclusion deformation was calculated, as shown in Figure 11. The conversion ratio was affected by the melting time, inclusion type, and size. The conversion ratio increased quickly at the beginning of the modification but became slow as the reaction progressed. It can be seen that when the conversion ratio of CA to $C_{12}A_7$ with a 2 μm radius increased from 0% to 57.8%, this took 167 s, while the time needed to prolong the process was 902 s, with a conversion ratio increase from 57.8% to 100%; it took about six times longer time at the later stage of inclusion modification than at the early stage. Therefore, in the later stage of inclusion modification, the stirring speed should be increased to promote inclusion modification and reduce the modification time.

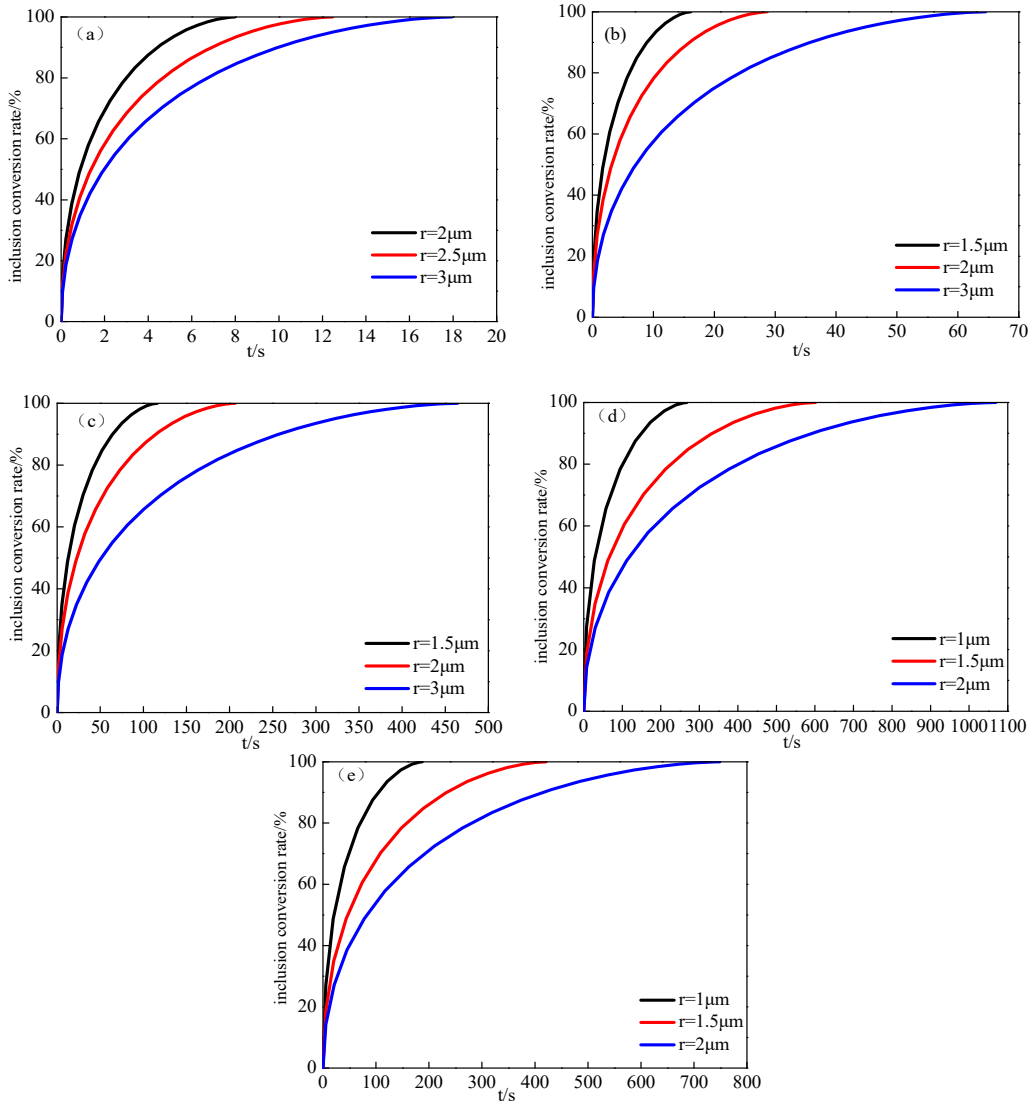

Figure 11. Modification process of inclusions with different particle sizes (**a**) Al_2O_3 is modified into CA6, (**b**) CA_6 is modified into CA_2, (**c**) CA_2 is modified into CA, (**d**) CA is modified into $C_{12}A_7$, (**e**) $C_{12}A_7$ is modified into C_3A).

4.6. Relationship between Inclusion Radius and Modification Time

The relationship between the inclusion radius and modification time was studied based on Equation (12), as shown in Figure 12. The complete modification times for inclusions increased with the square of their radii. The complete modification time was prolonged by four times, while the radii of unmodified inclusions doubled. The complete modification time for inclusions with a 1 μm radius from CA to $C_{12}A_7$ was 267 s, and was 1069 s for inclusions with a 2 μm radius. During the whole modification process of solid Al_2O_3 inclusions to liquid calcium aluminate inclusions of the same size, the modification time for inclusions from CA to $C_{12}A_7$ was the longest.

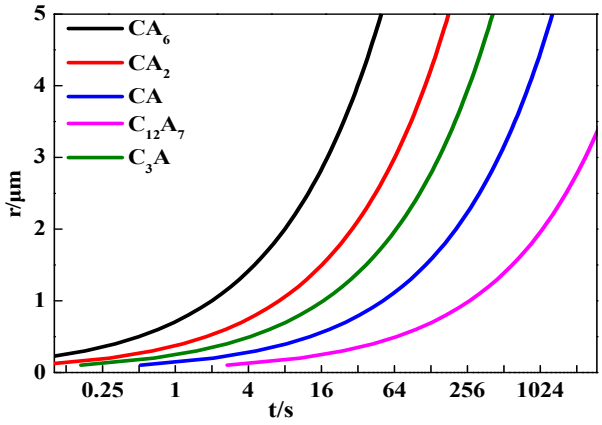

Figure 12. Complete modification time for Al_2O_3 inclusions of different sizes.

4.7. Modeling Verification

In order to verify the calculation of the kinetic model for the modification of Al_2O_3 inclusions during calcium treatment, the calculated CaO content was compared with experimental results, considering the boundary conditions and unreacted core model parameters, as shown in Figure 13. The modification of inclusions with radii of 1, 2, and 3 μm was simulated based on observed results in experiments. It can be seen that the modification of Al_2O_3 inclusions in sample A is much faster than that in sample B, which is consistent with experimental results. The model calculation is closer to the experimental data, indicating that they are in good agreement. Additionally, it was found that the inclusions with 1 μm evolving from Al_2O_3 to CA_6 took no longer than 1 s. It took about 1000 s for inclusions with a 3 μm radius to modify Al_2O_3 into liquid calcium aluminate in sample A and about 6000 s for that in sample B.

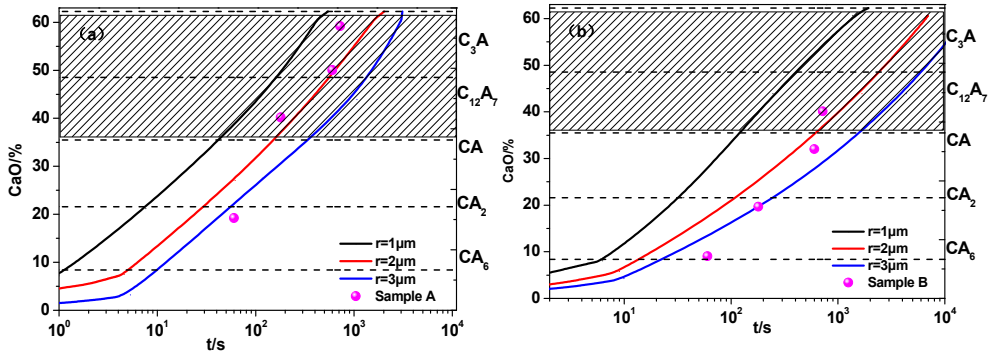

Figure 13. Variation of CaO contents in inclusions with time: (**a**) sample A; (**b**) sample B.

5. Conclusions

In the experiments with high-carbon hard wire steels treated with different contents of calcium at 1600 °C, the compositions and morphological evolution of inclusions were studied. The kinetic model for modification of Al_2O_3 inclusions during calcium treatment in high-carbon hard wire steels was established based on unreacted core theory. This model considers the transfer of Ca and Al through the boundary layer and within the product layer coupled with thermodynamic equilibrium at the interfaces. The calculated results based on the kinetic model were compared with experimental results. The main findings are summarized below:

1. The diffusion of Al in the inclusion layer was the limiting link in the inclusion modification process. The modification time increased linearly with increasing oxygen content and decreased with increasing calcium content in molten steel. The change of

modification time with increasing Al content was very small. The Ca concentration in molten steel had the greatest influence on the modification time of inclusions;

2. The modification times for inclusions tended to be longer in the transformation of higher CaO-containing calcium aluminate. The modification of Al_2O_3 into CA_6 was fastest, while the most time was needed to modify CA into $C_{12}A_7$;
3. It took about six times time longer at the later stage of inclusion modification than at the early stage. The complete modification times for inclusions increased with the square of their radii. The complete modification times were prolonged by four times when the radii of unmodified inclusions doubled;
4. The model calculation was in good agreement with experimental results. The inclusions with a 1 μm radius evolving from Al_2O_3 to CA_6 took no longer than 1s. The modification of Al_2O_3 inclusions in sample A was much faster than in sample B. It took about 1000 s for inclusion with a 3 μm radius to modify Al_2O_3 into liquid calcium aluminate in sample A and about 6000 s for that in sample B.

Author Contributions: Conceptualization: Z.X. and C.L.; Methodology: Z.X. and L.W.; Software: Z.X.; Writing—original draft preparation: Z.X. and L.W.; Writing—review and editing: C.L. and L.W. Funding acquisition: C.L. and L.W. All authors have read and agreed to the published version of the manuscript.

Funding: This project was supported by the National Science Foundation of China through grant numbers 51864013, 51804086, 52064011, and 52074095.

Institutional Review Board Statement: Not applicable.

Informed Consent Statement: Not applicable.

Data Availability Statement: Data is contained within the article.

Conflicts of Interest: The authors declare no conflict of interest.

References

1. Li, X.D.; Deng, S.; Yang, Y.B. Production practice of plasticity control of inclusions in CaO–Al_2O_3–SiO_2 system of SWRH82B hard wire steel. *Metall. China* **2018**, *28*, 61–66.
2. Elwazri, A.; Wanjara, P.; Yue, S. Measurement of pearlite interlamellar spacing in hypereutectoid steels. *Mater. Charact.* **2005**, *54*, 473–478. [CrossRef]
3. Tanaka, Y.; Pahlevani, F.; Kitamura, S.-Y.; Privat, K.; Sahajwalla, V. Behaviour of Sulphide and Non-alumina-Based Oxide Inclusions in Ca-Treated High-Carbon Steel. *Met. Mater. Trans. A* **2020**, *51*, 1384–1394. [CrossRef]
4. Atienza, J.M.; Elices, M.; Ruiz-Hervias, J.; Caballero, L.; Valiente, A. Residual stresses and durability in cold drawn eutectoid steel wires. *Met. Mater. Int.* **2007**, *13*, 139–143. [CrossRef]
5. Handoko, W.; Anurag, A.; Pahlevani, F. Effect of selective-precipitations process on the corrosion resistance and hardness of dual-phase high-carbon steel. *Sci. Rep.* **2019**, *9*, 15631. [CrossRef] [PubMed]
6. Wang, G.D.; Lv, Y.W. Research on inclusion control and rolling process optimization of 82B hard wire steel. *Metall. China* **2012**, *22*, 15–17, 21.
7. Robinson, S.W.; Martin, I.W.; Pickering, F.B. Formation of alumina in steel and its dissemination during mechanical working. *Metals Technol.* **1979**, *6*, 157–169. [CrossRef]
8. Jiang, Z.; Tieu, A.; Zhang, X.; Lu, C.; Sun, W. Finite element simulation of cold rolling of thin strip. *J. Mater. Process. Technol.* **2003**, *140*, 542–547. [CrossRef]
9. Abraham, S.; Bodnar, R.; Raines, J. Inclusion engineering and metallurgy of calcium treatment. *J. Iron. Steel. Res. Int.* **2018**, *1*, 1243–1257. [CrossRef]
10. Verma, N.; Pistorius, P.C.; Fruehan, R.J.; Potter, M.; Lind, M.; Story, S. Transient Inclusion Evolution During Modification of Alumina Inclusions by Calcium in Liquid Steel: Part I. Background, Experimental Techniques and Analysis Methods. *Metall. Mater. Trans. B.* **2011**, *42*, 711–719. [CrossRef]
11. Yang, G.W.; Wang, X.H.; Huang, F.X. Influence of Calcium Addition on Inclusions in LCAK Steel with Ultralow Sulfur Content. *Metall. Mater. Trans. B* **2015**, *46*, 145–154. [CrossRef]
12. Zhang, L.; Liu, Y.; Zhang, Y. Transient Evolution of Nonmetallic Inclusions During Calcium Treatment of Molten Steel. *Metall. Mater. Trans. B* **2018**, *49*, 1–19. [CrossRef]
13. Lamut, J.; Falkus, J.; Jurjevec, B. Influence of Inclusions Modification on Nozzle Clogging. *Arch. Metall. Mater.* **2012**, *57*, 319–324. [CrossRef]

14. Zheng, H.-Y.; Guo, S.-Q.; Qiao, M.-R.; Qin, L.-B.; Zou, X.-J.; Ren, Z.-M. Study on the modification of inclusions by Ca treatment in GCr18Mo bearing steel. *Adv. Manuf.* **2019**, *7*, 438–447. [CrossRef]
15. Holappa, L.; Hämäläinen, M.; Liukkonen, M.; Lind, M. Thermodynamic examination of inclusion modification and precipitation from calcium treatment to solidified steel. *Ironmak. Steelmak.* **2003**, *30*, 111–115. [CrossRef]
16. Xu, J.; Huang, F.; Wang, X. Formation Mechanism of CaS–Al_2O_3 Inclusions in Low Sulfur Al-Killed Steel After Calcium Treatment. *Metall. Mater. Trans. B* **2016**, *47*, 1217–1227. [CrossRef]
17. Lu, D.; Irons, G.A.; Lu, W. Kinetics and mechanisms of calcium dissolution and modification of oxide and sulphide inclusions in steel. *Ironmak. Steelmak.* **1994**, *21*, 362–372.
18. Higuchi, Y.; Numata, M.; Fukagawa, S.; Shinme, K. Inclusion Modification by Calcium Treatment. *ISIJ Int.* **1996**, *36*, S151–S154. [CrossRef]
19. Visser, H.-J.; Boom, R.; Biglari, M. Simulation of the calcium treatment of aluminium killed steel. *Rev. Métall.* **2008**, *105*, 172–180. [CrossRef]
20. Ito, Y.I.; Suda, M.; Kato, Y.; Nakato, H. Kinetics of Shape Control of Alumina Inclusions with Calcium Treatment in Line Pipe Steel for Sour Service. *ISIJ Int.* **1996**, *36*, S148–S150. [CrossRef]
21. Han, Z.; Liu, L.; Lind, M. Holappa Mechanism and Kinetics of Transformation of Alumina Inclusions by Calcium Treatment. *Acta. Metall. Sin.* **2006**, *19*, 1–8. [CrossRef]
22. Park, J.H.; Lee, S.-B.; Kim, D.S. Inclusion control of ferritic stainless steel by aluminum deoxidation and calcium treatment. *Met. Mater. Trans. A* **2005**, *36*, 67–73. [CrossRef]
23. Galindo, A.; Irons, G.; Sun, S. Modeling of the Trajectory of Slag and Metal Chemistry during Ladle Treatment Used to Predict Changes in the Primary Inclusion Type. In Proceedings of the International Congress on the Science & Technology of Steelmaking, Beijing, China, 12–14 May 2015.
24. Tabatabaei, Y.; Coley, K.S.; Irons, G.A.; Sun, S. A Multilayer Model for Alumina Inclusion Transformation by Calcium in the Ladle Furnace. *Metall. Mater. Trans. B* **2018**, *49*, 375–387. [CrossRef]
25. Turkdogan, E.T. *Proceedings of 1st International Calcium Treatment Symposium, University of Strathclyde, Glasgow, Scotland, 1988*; The Institute of Metals: London, UK, 1988; pp. 3–13.
26. Ye, G.; Jönsson, P.; Lund, T. Thermodynamics and Kinetics of the Modification of Al_2O_3 Inclusions. *ISIJ Int.* **1996**, *36*, S105–S108. [CrossRef]
27. Lei, H.; He, J.C. Mathematical Models on Inclusion Dynamics Behavior in the Molten Steel. *Chin. J. Process Eng.* **2010**, *10*, 288–292.
28. Min, Y.; Zhang, Q.; Xu, H.; Xu, J.; Liu, C. Formation and Evolution of Inclusions with Different Adding Order of Magnesium and Sulfur in Al-Killed Free-Cutting Steel. *Metals* **2018**, *8*, 1064. [CrossRef]
29. Tabatabaei, Y.; Coley, K.S.; Irons, G.A.; Sun, S. A Kinetic Model for Modification of $MgAl_2O_4$ Spinel Inclusions During Calcium Treatment in the Ladle Furnace. *Metall. Mater. Trans. B* **2018**, *49*, 2744–2756. [CrossRef]
30. Guo, J.; Cheng, S.S.; Cheng, Z.J. Kinetic modeling of alumina inclusion modification in Al – Killed steel after Ca treatment. *J. Univ. Sci. Technol. B* **2014**, *36*, 424–431.
31. Itoh, H.; Hino, M. Thermodynamics on the formation of spinel nonmetallic inclusion in liquid steel. *Metall. Mater. Trans. B* **1997**, *28*, 953–956. [CrossRef]
32. Wang, L.Z.; Yang, S.F.; Li, J.S. Effect of Mg Addition on the Refinement and Homogenized Distribution of Inclusions in Steel with Different Al Contents. *Metall. Mater. Trans. B* **2017**, *48*, 805–818. [CrossRef]